



LDL receptor and its family members serve as the cellular receptors for vesicular stomatitis virus

Danit Finkelshtein¹, Ariel Werman¹, Daniela Novick, Sara Barak, and Menachem Rubinstein²

Department of Molecular Genetics, The Weizmann Institute of Science, Rehovot 76100, Israel

Edited by Robert A. Lamb, Northwestern University, Evanston, IL, and approved March 21, 2013 (received for review August 23, 2012)

Vesicular stomatitis virus (VSV) exhibits a remarkably robust and pantropic infectivity, mediated by its coat protein, VSV-G. Using this property, recombinant forms of VSV and VSV-G-pseudotyped viral vectors are being developed for gene therapy, vaccination, and viral oncolysis and are extensively used for gene transduction in vivo and in vitro. The broad tropism of VSV suggests that it enters cells through a highly ubiquitous receptor, whose identity has so far remained elusive. Here we show that the LDL receptor (LDLR) serves as the major entry port of VSV and of VSV-G-pseudotyped lentiviral vectors in human and mouse cells, whereas other LDLR family members serve as alternative receptors. The widespread expression of LDLR family members accounts for the pantropism of VSV and for the broad applicability of VSV-G-pseudotyped viral vectors for gene transduction.

receptor-associated protein | virus entry | sLDLR

The enveloped RNA virus vesicular stomatitis virus (VSV) has been extensively studied and characterized (1, 2). This virus exhibits a remarkably robust and pantropic infectivity, mediated by its surface glycoprotein, VSV-G. VSV-G has been widely used for pseudotyping other viruses and viral vectors (1, 3–5). VSV-G-pseudotyped lentiviruses exhibit the same broad tropism as VSV, excellent stability, and high transduction efficiency, rendering them the gold standard for experimental gene transfer procedures. These and other VSV-G pseudotyped vectors are currently enabling effective gene therapy protocols for many human tissues (6–8).

The versatility of the VSV-G coat protein is not only exploited as a pseudotype gate opener for other viruses and viral vectors, but also in direct clinical applications of VSV in its native or engineered forms. The fact that VSV infects and lyses all transformed cell lines tested to date has been translated into protocols designed to target tumor cells for viral oncolysis. Unlike transformed cells, the innate intracellular antiviral state elicited by VSV in nontransformed cells leaves them unharmed (9). WT or engineered VSV has been shown to be efficacious in preclinical models against malignant glioma, melanoma, hepatocellular carcinoma, breast adenocarcinoma, selected leukemias, prostate cancer-based tumors, osteosarcoma, and others (10–14). The attributes of VSV-G have also been used to develop VSV-based vaccination protocols for tumor antigens, as well as for a range of pathogens (15), including influenza (1) and HIV, for which experiments with monkeys showed a great deal of promise (4, 16). Recently, recombinant VSV-based vaccination against tumor antigens was shown to cure established tumors (17).

To date, attempts to identify the VSV receptor on the cell membrane have been unsuccessful, and this has been a source of significant controversy. Genetic, biochemical, and immunochemical studies have shown that VSV-G is necessary for VSV binding to its putative receptor, its internalization, and its fusion with the target cell membrane (18–20). After binding, VSV undergoes clathrin-mediated endocytosis (21), indicating that it gains access to cells through binding of VSV-G to an as yet unidentified cellular receptor. Early studies reported that proteolytic digestion of the cell surface proteins did not affect VSV binding, suggesting that the cellular binding site of VSV is not a membrane protein (22). In line with these observations and with the wide tropism of VSV, its receptor was suggested to be a ubiquitous plasma membrane lipid

component, such as phosphatidylserine, phosphatidylinositol, or the ganglioside GM3 (23–25). Whereas many publications refer to phosphatidylserine as the VSV receptor, more recent studies demonstrated that this membrane component is not the cell surface receptor for VSV (26, 27).

Previously we reported that IFN-treated cells secrete a soluble form of the LDL receptor (sLDLR), contributing to inhibition of VSV infectivity (28). We further demonstrated that this receptor fragment is found naturally in body fluids (29). Here we show that the cell surface LDLR serves as the major cellular entry port of VSV and that other LDLR family members serve as alternative, albeit less effective, entry routes in human and mouse cells.

Results

Soluble LDLR Inhibits VSV Infectivity by Binding to VSV. Initially we confirmed our previously reported observation that sLDLR inhibits VSV infectivity (28); to this end, we used highly purified (Fig. 1A, *Inset*) recombinant human sLDLR, consisting of seven cysteine-rich repeats, which correspond to the ligand-binding domain of LDLR (30). Recombinant sLDLR inhibited the VSV-triggered cytopathic effect in human epithelial WISH cells in a dose-dependent manner, with an IC_{50} of 55 ng/mL (~0.4 nM; Fig. 1A). Similar results were obtained with mandarin darby bovine kidney (MDBK) cells, and mouse L cells (Fig. 1B). Exposure of cells to as little as 0.1 multiplicity of infection (MOI) of VSV for only 5 min was sufficient to trigger a complete cytopathic effect at 17 h after infection (Fig. 1C, well “V”), indicating that the majority of the cell lysis was due to secondary infection by the VSV progeny. Addition of sLDLR before or concomitantly with VSV completely blocked the VSV-triggered cytopathic effect, whereas its addition 5–10 min after VSV challenge partly inhibited only the secondary infection, resulting in a plaque-like appearance (Fig. 1C). In contrast, removal of sLDLR before virus challenge resulted in a near complete cytopathic effect (Fig. 1C, well “R”). These results indicated that to exert its antiviral effects, sLDLR must be present both at the early stages of the viral infection and at later stages, to also inhibit secondary infection by viral progeny. To test whether sLDLR inhibits the initial binding of VSV to cells, we exposed WISH cells to VSV for 15 min in the absence or presence of sLDLR, then washed the cells and measured cell-associated VSV by quantitative and by semiquantitative RT-PCR of VSV RNA. We found that sLDLR inhibited VSV binding to cells in a dose-dependent manner, at both 4 °C and 37 °C (Fig. 1D, *Inset*).

The inhibition of virus–cell binding mediated by sLDLR suggested that sLDLR inhibits VSV infectivity by binding to either the virus or to a putative cellular VSV receptor. To test the

Author contributions: D.F., A.W., D.N., and M.R. designed research; D.F., D.N., and S.B. performed research; D.F., D.N., and M.R. analyzed data; and M.R. wrote the paper.

The authors declare no conflict of interest.

This article is a PNAS Direct Submission.

¹D.F. and A.W. contributed equally to this work.

²To whom correspondence should be addressed. E-mail: menachem.rubinstein@weizmann.ac.il.

This article contains supporting information online at www.pnas.org/lookup/suppl/doi:10.1073/pnas.1214441110/-DCSupplemental.

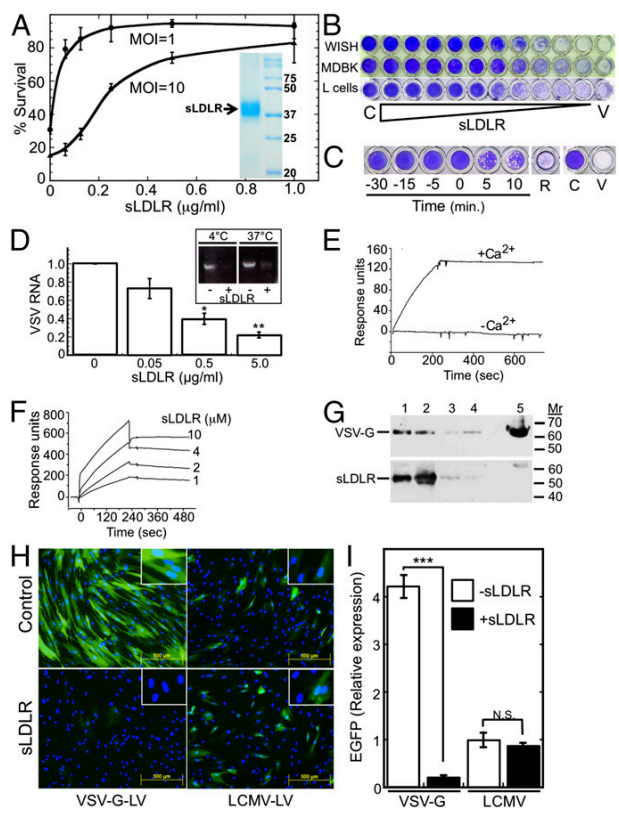


Fig. 1. Soluble LDLR binds VSV and inhibits infection by VSV and transduction by a VSV-G-pseudotyped lentiviral vector. (A) Survival \pm SD of WISH cells as determined by Neutral red staining after treatment with sLDLR and challenge by VSV at the indicated MOI. $n = 3$. (Inset) SDS/PAGE of sLDLR (10 μ g). Molecular mass markers (kDa) are shown on the right lane. (B) Surviving WISH cells, bovine MDBK cells, and murine L cells after treatment with serially twofold-diluted sLDLR (starting at 8 μ g/ml) followed by VSV (MOI = 1 for WISH and MDBK cells, MOI = 0.07 for L cells). C, no virus; V, VSV without sLDLR. (C) Surviving WISH cells after addition of sLDLR (1 μ g/ml) at the indicated times relative to the time of VSV (MOI = 0.1) addition. In well R, sLDLR was added for 120 min and removed before VSV challenge. C and V are as in B. (D) Quantitative RT-PCR of VSV RNA after attachment of VSV (MOI = 10) at 4 $^{\circ}$ C for 4 h to WISH cells in the presence of the indicated sLDLR concentrations. VSV RNA \pm SE is normalized to TATA binding protein mRNA; * $P < 0.02$, ** $P < 0.002$, compared with the leftmost bar, $n = 3$. (Inset) RT-PCR products of VSV RNA, isolated after similar experiments, performed at 4 $^{\circ}$ C and at 37 $^{\circ}$ C. (E) Surface plasmon resonance analysis of VSV binding to immobilized sLDLR in PBS with or without CaCl_2 (1 mM). (F) Surface plasmon resonance analysis of sLDLR binding to immobilized VSV-G-LV in PBS + 1 mM CaCl_2 . (G) (Upper) Immunoblotting of VSV-G after coimmunoprecipitation of a solubilized VSV-sLDLR complex with the following antibodies (lanes): 1, mAb 28.28 anti-LDLR; 2, mAb C7 anti-LDLR; 3, isotype control mAb; 4, no antibody. A VSV-G marker is shown in lane 5. (Lower) Reblotting of the membrane with anti-LDLR mAb 29.8. (H) EGFP expression (green) after transduction of FS-11 fibroblasts with either EGFP-encoding VSV-G-LV or EGFP-encoding LCMV-LV in the presence or absence of sLDLR (5 μ g/ml). Nuclei were counterstained with Hoechst 33258 (blue). (Insets) Enlarged magnifications. (I) Average \pm SD EGFP expression in cultures transfected as shown in H. *** $P < 0.003$, $n = 4$. N.S., not significant ($P = 0.525$), $n = 4$.

possible binding of sLDLR to VSV, we used surface plasmon resonance. Binding of LDL to LDLR is Ca^{2+} dependent (31). Similarly, we found that VSV effectively bound to immobilized sLDLR in PBS, but only in the presence of Ca^{2+} (Fig. 1E). Because the VSV envelope contains 400–500 trimeric VSV-G spikes, quantitative analysis of its binding to immobilized sLDLR

reflects avidity rather than affinity. Dose–response binding of VSV to immobilized sLDLR gave a dissociation constant (K_d) of 10^{-11} M, indicating a very high avidity (Fig. S1). VSV-G-pseudotyped lentiviral vectors (VSV-G-LV) share with VSV only their receptor-interacting component, VSV-G, and hence can be used for measuring the affinity of VSV-G to sLDLR. To this end we immobilized VSV-G-LV to the sensor chip and analyzed binding of increasing sLDLR concentrations in the presence of Ca^{2+} . As expected, the affinity of a single sLDLR molecule interacting with VSV-G ($K_d = 10^{-8}$ M; Fig. 1F) was lower than the avidity measured by VSV binding to immobilized sLDLR. In a control experiment we tested binding of sLDLR to immobilized lymphocytic choriomeningitis virus-pseudotyped lentiviral vector (LCMV-LV), which differs from VSV-G-LV only in its coat protein. sLDLR did not bind to the immobilized LCMV-LV. The high affinity of the VSV binding to sLDLR and the dependence of the binding on Ca^{2+} strongly supported the specificity and physiological relevance of this *in vitro* interaction. Further evidence for the interaction between the ligand-binding domain of LDLR and VSV-G was obtained by coimmunoprecipitation. sLDLR was added to a suspension of VSV and then immunoprecipitated with protein-G-bound anti-LDLR mAb 28.28 (32), anti-LDLR mAb C7, an isotype-matched control mAb, or no antibody. SDS/PAGE and immunoblotting with anti-VSV-G and anti-LDLR antibodies revealed that sLDLR was specifically bound to VSV-G (Fig. 1G).

We also evaluated the impact of sLDLR on EGFP expression after transduction of cells with an EGFP-encoding VSV-G-LV. Figs. 1H and I show that sLDLR completely blocked transduction of newborn human FS-11 foreskin fibroblasts by EGFP-encoding VSV-G-LV. In contrast, sLDLR did not inhibit transduction of the cells with an EGFP-encoding LCMV-LV, which differs from VSV-G-LV only by its coat protein. Taken together, these results indicate that sLDLR inhibits VSV infectivity by binding to VSV-G.

LDLR Is the Major VSV Receptor in Human Cells. The fact that sLDLR bound VSV at high affinity and inhibited its infectivity indicated that sLDLR masked VSV constituents essential for its interaction with a cellular receptor, prompting us to examine whether LDLR serves as the VSV entry port. On the basis of increased binding of radiolabeled VSV to trypsin-treated cells, earlier studies concluded that the VSV receptor was unlikely to be a protein (22, 33). To examine this conclusion more rigorously, we tested trypsin-treated cells for their resistance to VSV infection. We exposed these cells in suspension to trypsin/EDTA or to EDTA alone for 30 min, then washed the cells three times with medium containing 10% (vol/vol) FBS to block residual trypsin activity, as described previously (22). We then challenged the cell suspensions with VSV, washed the cells, plated them, and incubated them for 17 h. The EDTA-treated cells were completely lysed by VSV, whereas the trypsin-treated cells were fully resistant to VSV infection (Fig. 2A, Upper). Plaque assays of the culture supernatants revealed \sim 500-fold lower VSV yields in the trypsin-treated cultures (Fig. 2A, Lower). These results indicate that a cell surface protein is essential for VSV infectivity, probably serving as a VSV receptor.

We then examined whether VSV and LDL, the physiological LDLR ligand, compete for binding to LDLR. FS-11 fibroblasts were incubated with increasing concentrations of VSV, followed by fluorescently labeled LDL (DiI-LDL) (4 h, 4 $^{\circ}$ C). The cultures were then washed and brought to 37 $^{\circ}$ C for 1 h to allow internalization of the bound DiI-LDL. VSV inhibited binding of DiI-LDL to the FS-11 fibroblasts in a dose-dependent manner (Fig. 2B). No uptake was seen when DiI-LDL alone was similarly incubated with the LDLR-deficient (34) GM701 fibroblasts (Fig. 2C). Similarly, VSV inhibited DiI-LDL binding to FS-11 fibroblasts, as determined by flow cytometry (Fig. 2D). These results indicate that VSV and LDL share LDLR as their common receptor. However, as we reported previously (28), LDLR-deficient

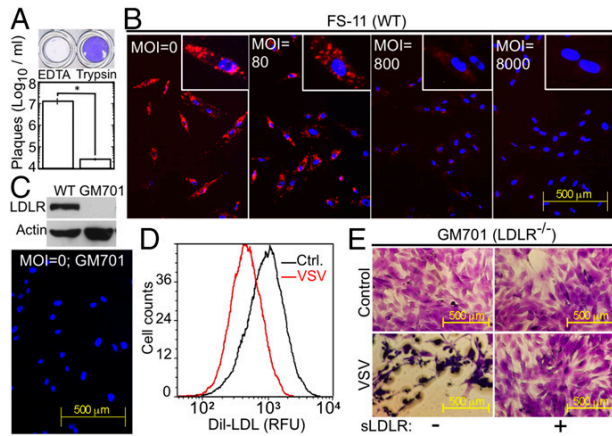


Fig. 2. VSV and LDL share a common cell surface receptor. (A) Surviving WISH epithelial cells, pretreated with trypsin-EDTA or EDTA, washed and challenged with VSV (0.015 MOI, 15 min). Figure is representative of six replicates. VSV yield (Lower) was determined by a plaque assay of the culture supernatants. * $P < 0.03$, $n = 3$. (B) Internalized Dil-LDL (red) in FS-11 fibroblasts after binding (1.67 $\mu\text{g}/\text{mL}$, 4 h, 4 $^{\circ}\text{C}$) in the presence of the indicated VSV MOI. The cultures were then washed, and bound Dil-LDL was allowed to internalize (1 h, 37 $^{\circ}\text{C}$). (Insets) Higher magnifications. (C) (Upper) Immunoblot of LDLR in WT FS-11 fibroblasts and LDLR-deficient GM701 fibroblasts. (Lower) Lack of Dil-LDL uptake by LDLR-deficient GM701 fibroblasts. (D) Flow cytometry of FS-11 fibroblasts treated with Dil-LDL as in A in the absence or presence of VSV (MOI = 2000). $n = 3$. (E) LDLR-deficient GM701 fibroblasts untreated or treated with sLDLR (1 $\mu\text{g}/\text{mL}$) and challenged with VSV (MOI = 1).

fibroblasts were not resistant to VSV infection, suggesting the existence of additional VSV receptors (Fig. 2E).

To obtain further evidence that LDLR is a VSV receptor, we used mAbs raised against epitopes within the ligand-binding domain of human LDLR (32). Because LDLR-deficient cells were still susceptible to VSV infection (Fig. 2E), we resorted to limited infection, thereby rendering the cell surface receptor the rate-limiting component. We incubated WISH cells with anti-LDLR mAbs for 30 min at 4 $^{\circ}\text{C}$, followed by VSV challenge (MOI = 0.05, 4 $^{\circ}\text{C}$, 1 h). The cultures were washed and then incubated for 17 h at 37 $^{\circ}\text{C}$ in the presence of the same antibodies. mAb 29.8, directed against class A cysteine-rich repeat 3 of the LDLR ligand-binding domain, almost completely inhibited the VSV-triggered cytopathic effect in WISH cells, whereas mAb 28.28, directed against repeat 6, did not inhibit VSV infectivity (Fig. 3A). Using the same infection protocol revealed that mAb 29.8 almost completely inhibited the VSV-triggered cytopathic effect in WT FS-11 fibroblasts but not in the LDLR-deficient GM701 fibroblasts (Fig. 3B). These experiments indicate that LDLR is the major VSV receptor in human cells, and VSV requires cysteine-rich repeat 3 of the LDLR ligand-binding domain to infect human cells; furthermore, it is likely that VSV uses alternative entry port(s) in the LDLR-deficient cells.

Other LDLR Family Members Serve as Alternative VSV Entry Ports.

The ligand-binding domain of all LDLR family members contains multiple, class A cysteine-rich repeats, structurally homologous to those of the LDLR (35). Because sLDLR completely blocked VSV infectivity even in LDLR-deficient cells (Fig. 2E), we hypothesized that such additional family members could serve as the alternative VSV entry routes. Receptor-associated protein (RAP) is a common chaperone of all LDLR family members (35). When added exogenously, RAP completely blocks ligand binding to all LDLR family members with the exception of LDLR itself (36). Indeed, preincubation of cells with RAP inhibited the VSV-triggered cytopathic effect in LDLR-deficient GM701 fibroblasts

but not in LDLR-expressing WT FS-11 fibroblasts (Fig. 3C). Similarly, measuring virus yields 7 h after infection revealed that LDLR-deficient GM701 fibroblasts were significantly less susceptible to VSV infection compared with WT fibroblasts (Fig. 3D). Importantly, RAP further attenuated VSV expression in the LDLR-deficient fibroblasts but not in the WT cells (Fig. 3D).

We then studied the impact of blocking all LDLR family members on VSV infectivity by combining RAP and anti-LDLR antibodies. We preincubated WISH cells either with the neutralizing or the nonneutralizing anti-LDLR mAbs, 29.8 and 28.28, in the absence or presence of RAP at 37 $^{\circ}\text{C}$ and then challenged the cells with VSV. RAP alone provided little protection from VSV infection, and nonneutralizing mAb 28.28 provided no protection, whereas anti-LDLR mAb 29.8 provided limited but significant protection. However, the combination of RAP and mAb 29.8, which blocks all LDLR family members, completely inhibited VSV infection (Fig. 3E).

We then studied the role of the LDLR family members in VSV uptake. WT and LDLR-deficient fibroblasts were incubated with VSV at conditions leading to internalization of at least two-thirds

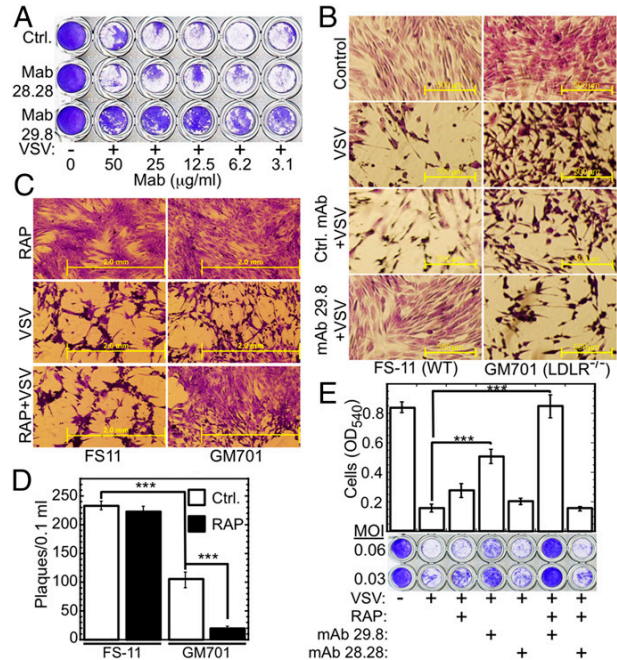


Fig. 3. LDLR and its family members are the major and the alternative VSV receptors, respectively. (A) Crystal violet-stained WISH cells, untreated (Ctrl.) or treated with anti-LDLR mAbs (30 min, 4 $^{\circ}\text{C}$) and then subjected to limited infection by VSV (MOI = 0.05, 4 $^{\circ}\text{C}$, 1 h). (B) Crystal violet-stained cultures of WT (FS-11) and LDLR-deficient (GM701) fibroblasts, either untreated (Control) or treated with isotype control mAb or anti-LDLR mAb 29.8 (12.5 $\mu\text{g}/\text{mL}$ each), followed by VSV as in A. (C) Crystal violet-stained cultures of WT FS-11 fibroblasts and LDLR-deficient GM701 fibroblasts, treated with RAP (100 nM, 30 min, 37 $^{\circ}\text{C}$) alone, VSV (MOI = 1) alone, or RAP followed by VSV. (D) Plaque assay of culture supernatants from WT FS-11 fibroblasts and LDLR-deficient GM701 fibroblasts (50,000 cells per well) preincubated (30 min, 37 $^{\circ}\text{C}$) in DMEM-10 or in DMEM-10 + RAP (100 nM), then challenged with VSV (0.5 MOI, 30 min, 37 $^{\circ}\text{C}$), washed three times, and incubated in DMEM-10 (0.1 mL, 37 $^{\circ}\text{C}$, 7 h). *** $P < 0.001$, $n = 4$. (E) Crystal violet-stained WISH cells grown to confluence in 96-well plates, incubated (30 min, 37 $^{\circ}\text{C}$) with the indicated combinations of RAP (200 nM), neutralizing anti-LDLR mAb 29.8, and nonneutralizing anti-LDLR mAb 28.28 (50 $\mu\text{g}/\text{mL}$ each); cells were then challenged with VSV at the indicated MOI. Cell viability (bar plot) was determined by reading the OD₅₄₀ of cultures treated with VSV at MOI = 0.06. *** $P < 0.002$, $n = 4$.

of the bound VSV (37). The cultures were then washed, immunostained with anti-VSV-G, and VSV foci were counted. Compared with the WT FS-11 fibroblasts, the LDLR-deficient GM701 fibroblasts internalized significantly less VSV (Figs. 4 *A* and *C*). This result confirmed that LDLR has a major role in VSV internalization. Furthermore, neutralizing mAb 29.8 but not the nonneutralizing mAb 28.28 significantly inhibited VSV binding and subsequent internalization into the WT fibroblasts ($P < 0.05$), whereas the combination of mAb 29.8 and RAP, which blocks all LDLR family members, completely abolished VSV binding and subsequent internalization to these cells (Figs. 4 *B* and *C*). Hence, we concluded that LDLR and its other family members mediate VSV entry into human cells.

LDLR and Its Family Members Mediate Transduction by VSV-G-Pseudotyped Lentiviral Vectors. VSV and the frequently used VSV-G-LVs share VSV-G as their common coat protein, prompting us to study the role of LDLR and its family members in cell transduction by an EGFP-encoding VSV-G-LV. After transduction, WT FS-11 fibroblasts expressed significantly higher levels of EGFP compared with LDLR-deficient fibroblasts (Fig. 5 *A* and *B*). To demonstrate that the reduced EGFP expression in the LDLR-deficient fibroblasts was due to lack of LDLR and not due to other inherent difference between these two cell types, we performed two control experiments. First we transduced both the WT and the LDLR-deficient fibroblasts with EGFP-encoding VSV-G-LV in the presence of polybrene, an agent rendering virus entry receptor-independent (38). Under these conditions, the level of EGFP expression in the WT and the LDLR-deficient GM701 fibroblasts was comparable (Fig. 5 *A* and *B*). Furthermore, transduction with another lentiviral vector, EGFP-encoding LCMV-LV, which differs from VSV-G-LV only in its coat protein, gave very similar levels of EGFP expression in the WT and LDLR-deficient fibroblasts (Fig. 5 *A* and *C*). These two control experiments confirmed that the reduced level of EGFP expression observed in the GM701 fibroblasts after transduction with VSV-G-LV was due to their lack of LDLR expression.

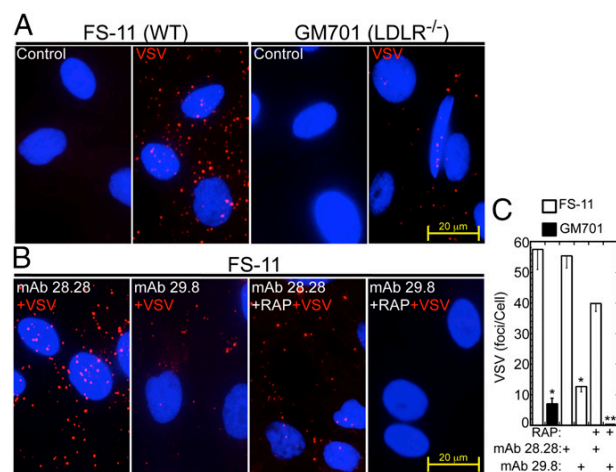


Fig. 4. LDLR and its family members mediate VSV internalization by human fibroblasts. (A) Internalized VSV in WT FS-11 fibroblasts and LDLR-deficient GM701 fibroblasts after incubation with VSV (MOI = 500, 4 min, 37 °C) and washing three times with PBS. The cultures were then fixed and stained with anti-VSV-G (red). (B) Internalized VSV in WT FS-11 fibroblasts preincubated with the indicated combinations of RAP and anti-LDLR mAbs (30 min, 37 °C), followed by VSV as in A. (C) VSV foci in A and B were counted in fields containing at least 30 cells. $**P < 0.01$; $*P < 0.05$ (compared with FS-11 challenged with VSV only, leftmost bar); $n = 3$.

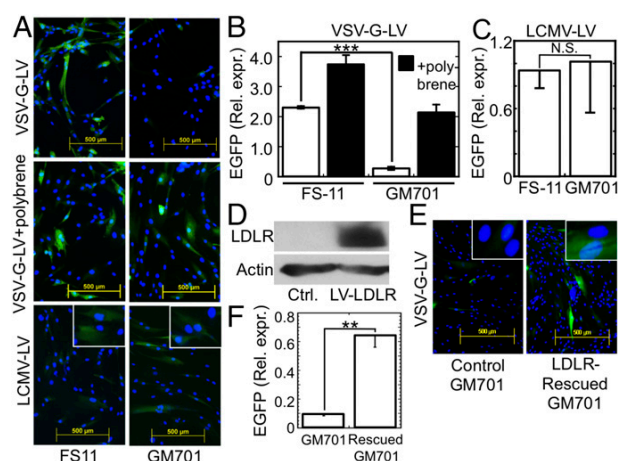


Fig. 5. LDLR is the main entry port of VSV-G-LV. (A) EGFP expression in WT FS-11 fibroblasts and LDLR-deficient GM701 fibroblasts, 72 h posttransduction with either EGFP-encoding VSV-G-LV in the absence or presence of polybrene, or with EGFP-encoding LCMV-LV in the absence of polybrene. (Insets) Higher magnifications. (B) Average \pm SD of the relative EGFP expression (Rel. expr.) after transduction with VSV-G-LV in the absence (open bars) or presence (filled bars) of polybrene. $***P < 0.0001$, $n = 3$. (C) Average \pm SD of the relative EGFP expression after transduction with LCMV-LV. N.S., not significant ($P = 0.78$), $n = 3$. (D) Immunoblot of LDLR after either mock transduction of GM701 fibroblasts with polybrene alone (Ctrl.) or their transduction with VSV-G-LV encoding LDLR in the presence of polybrene (LV-LDLR). (E) EGFP expression in cultures of LDLR-reconstituted or mock-transduced GM701 fibroblasts, transduced for 48 h with EGFP-encoding VSV-G-LV. (Insets) Higher magnifications. (F) Average \pm SD of the relative EGFP expression shown in E. $**P < 0.01$, $n = 3$.

To further confirm the role of LDLR in VSV-G-LV entry to cells, we rescued LDLR expression in the LDLR-deficient GM701 fibroblasts by polybrene-assisted transduction with an LDLR-encoding VSV-G-LV. After rescue, the GM701 cells expressed LDLR, as determined by immunoblotting (Fig. 5*D*), and became significantly more responsive to transduction with the EGFP-encoding VSV-G-LV in the absence of polybrene (Fig. 5*E* and *F*). In a reciprocal experiment, knockdown of *LDLR* by specific siRNA and not by scrambled, nontargeting control siRNA significantly attenuated the transduction of FS-11 fibroblasts by VSV-G-LV, whereas it had no significant effect on transduction of the cells by LCMV-LV (Fig. S2). This study further confirmed that the reduced transduction by VSV-G-LV observed in the LDLR-deficient cells was due to lack of LDLR and not due to other inherent differences between the WT FS-11 fibroblasts and the LDLR-deficient GM701 cells.

We then studied whether other LDLR family members enable transduction of cells by VSV-G-LV. As was the case with VSV infection (Fig. 3*C–E*), RAP further attenuated the transduction of the LDLR-deficient GM701 fibroblasts by VSV-G-LV, indicating that in addition to LDLR, other LDLR family members enabled the residual transduction observed in the LDLR-deficient fibroblasts (Fig. 6*A* and *B*). In parallel, we found that similarly to human cells, LDLR-deficient murine embryonic fibroblasts (MEFs) were significantly less susceptible to transduction by VSV-G-LV compared with their WT counterparts, and RAP further attenuated the VSV-G-LV-mediated transduction of the LDLR-deficient MEFs. Unlike human fibroblasts, RAP significantly reduced VSV infectivity of WT MEFs (Fig. 6*C* and *D*), suggesting a more substantial role of the other LDLR family members in VSV infection of mouse cells.

Taken together, our results demonstrate that LDLR is the major entry port of both VSV and VSV-G-LVs in human and mouse cells, whereas other LDLR family members serve as

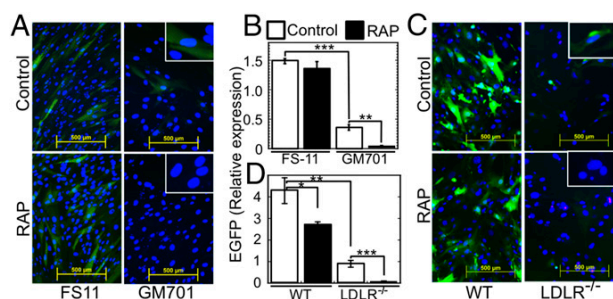


Fig. 6. Other LDLR family members are alternative entry ports of VSV-G-LV in human and mouse cells. (A) EGFP expression in WT FS-11 fibroblasts and LDLR-deficient GM701 fibroblasts, transduced with EGFP-encoding VSV-G-LV in the absence (Control) or presence of RAP (100 nM). (Insets) Higher magnifications. (B) Average \pm SD of EGFP expression shown in A. $***P < 0.0002$, $n = 3$. $*P < 0.03$, $n = 3$. (C) EGFP expression in WT murine embryonic fibroblasts (WT) and LDLR-deficient MEFs, transduced with EGFP-encoding VSV-G-LV as in A. (Insets) Higher magnifications. (D) Average \pm SD of EGFP expression shown in C. All fluorescence intensity values were normalized to the nuclei counts. $*P < 0.05$, $**P < 0.007$, $***P < 0.002$, $n = 3$.

alternative receptors. The complete protection from VSV infection obtained by blocking all LDLR family members identifies these receptors as the only possible VSV entry ports into human cells.

Discussion

In this study we provide several lines of evidence establishing LDLR as the major entry port of VSV and VSV-G-LV, including the high affinity and calcium ion dependence of VSV binding to soluble LDLR, the competition between VSV and LDL for receptor binding, the inhibition of VSV internalization and infectivity by mAbs to the ligand-binding domain of LDLR, and the crucial role of LDLR in cell transduction by a VSV-G-LV. On the basis of binding of radiolabeled VSV to protease-treated cells, earlier studies proposed that the VSV receptor is not a protein (22, 24, 33). In contrast, our finding that such trypsin-treated cells resist VSV infection indicates that the VSV receptor is a protein. Two earlier studies indirectly support the role of LDLR as the major VSV receptor. Binding of VSV to MDCK epithelial cells is 100 times more prevalent at the basolateral membrane compared with their apical surface (39). Independently, it was shown that LDLR is expressed 100 times more efficiently on the basolateral surface of these MDCK cells (40).

The fact that LDLR-deficient fibroblasts were susceptible to VSV infection suggested the possible existence of alternative, albeit less-efficient virus entry routes. All LDLR family members contain conserved class A repeats in their ligand-binding domains, which is the same structural motif that we have identified as the VSV-binding epitope in LDLR. The ability of RAP, which blocks all LDLR family members except LDLR, to attenuate VSV infection of the LDLR-deficient fibroblasts indicates that the alternative VSV receptor is another member of the LDLR family. One possible candidate is LRP1, which is overexpressed in GM701 cells (41), possibly explaining why these fibroblasts were highly susceptible to limited VSV infection, whereas WT fibroblasts in which LDLR was blocked by a specific monoclonal antibody were fully protected under the same VSV challenge (Fig. 3B, Lower). Our observations that a combination of monoclonal anti-LDLR antibody and RAP abolished VSV binding and internalization and completely protected human cells from VSV infection (Figs. 3E and 4) indicate that VSV enters and infects human and mouse cells only through members of the LDLR family. LDLR family members are ubiquitously expressed in all cell types and across the animal kingdom (42), thereby providing the basis for the remarkable pantropism of VSV. Interestingly, however, we found that

sLDLR did not inhibit infection of insect SF6 cells. Although the insect lipophorin receptor and mammalian LDLR are structurally highly similar, their mode of action is quite different. Whereas LDLR releases its cargo in the endosome, lipophorin remains associated with its receptor and is eventually resecreted (43). Hence VSV probably infects insect cells by other means.

LDLR family proteins are endocytosed and recycle back to the membrane every 10 min, irrespective of ligand binding (44), and hence are ideal virus entry ports. It is therefore not surprising that in addition to VSV, several other unrelated viruses have been suggested to use these receptors as their ports of cellular entry (45–47). Of particular interest are the minor group common cold virus (46) and hepatitis C virus (48), which much like VSV use LDLR as well as other LDLR family members for cell entry. Similar to any other ligand, once internalized, VSV must dissociate from its receptor. The endosomal lumen is characterized by low pH and low concentration of calcium ions; both these features are required for β -VLDL release from LDLR (49). Our finding that Ca^{2+} is essential for binding of VSV to immobilized sLDLR in vitro suggests that calcium ion depletion might also facilitate VSV release from its receptor after internalization.

In recent years high-throughput genome-wide screens became the method of choice for deciphering gene function. However, such screens may fail in cases of genetic redundancy, and the VSV receptor is a good case in point. A recent study using genome-wide RNAi screen identified 173 host genes essential for completion of the VSV replication cycle, but it did not detect the VSV receptor despite its obviously essential role (50). Recently it was demonstrated that the endoplasmic reticulum chaperone gp96 (endoplasmic reticulum chaperone GRP94) is essential for VSV binding to cells and for their subsequent infection (27). This chaperone is a constituent of a multiprotein complex, required for protein folding in the endoplasmic reticulum (51). Grp78, another component of this multiprotein complex, was reported to interact with LDLR (52). In preliminary studies we found that knockdown of gp96 disrupted the glycosylation of LDLR, manifested by reduced apparent molecular mass in SDS/PAGE. It is therefore likely that processing of other LDLR family members, which serve as VSV receptors, also requires gp96, thereby explaining its critical role in VSV infectivity.

The identification of the VSV receptor is of significant clinical importance because recombinant VSV and VSV-G-pseudotyped viral vectors are being developed for viral oncolysis, for vaccination, and for gene therapy. Up-regulation of LDLR in vivo [e.g., by pretreatment with statins (53)] might increase the efficacy of such vectors. Furthermore, liver cells and certain tumor cells, which express high levels of LDLR (54), might be the preferred targets of VSV-G-based gene therapy as well as VSV-G-based viral oncolysis.

Materials and Methods

LDLR-deficient human GM701 fibroblasts were from the Coriell Institute. Human FS-11 foreskin fibroblasts were kindly provided by M. Revel. VSV (Indiana Strain) and all other cell types were from ATCC. Cells were grown in media containing 10% (vol/vol) FBS (MEM-10 or DMEM-10). VSV was propagated in WISH cells, purified by gradient centrifugation, and plaque-assayed. sLDLR_{25–313} was produced in CHO cells and purified to homogeneity. VSV cytopathic effects were evaluated 17 h after VSV challenge. Plaque assays, flow cytometry, preparation of lentiviral vectors, transduction of cells, RT-PCR, quantitative PCR, surface plasmon resonance, knockdown of LDLR mRNA, immunoblotting, and all other methods were performed according to published procedures or as recommended by the various manufacturers. Trypsin digestion was performed using cell culture grade trypsin/EDTA on cells in suspension. Residual trypsin activity was blocked by 3 \times washing of the cells in DMEM-10 before VSV challenge. Image analysis and counting of nuclei, plaques, and VSV foci was performed using the ImageJ program (National Institutes of Health). Fluorescence intensities and internalized VSV foci were normalized to the number of nuclei/field, using fields containing at least 30 nuclei. Statistical analysis was performed using the unpaired Student *t* test of the KaleidaGraph program on at least three independent replicates. Details can be found in *SI Materials and Methods*.

Explore Litigation Insights

Docket Alarm provides insights to develop a more informed litigation strategy and the peace of mind of knowing you're on top of things.

Real-Time Litigation Alerts



Keep your litigation team up-to-date with **real-time alerts** and advanced team management tools built for the enterprise, all while greatly reducing PACER spend.

Our comprehensive service means we can handle Federal, State, and Administrative courts across the country.

Advanced Docket Research



With over 230 million records, Docket Alarm's cloud-native docket research platform finds what other services can't. Coverage includes Federal, State, plus PTAB, TTAB, ITC and NLRB decisions, all in one place.

Identify arguments that have been successful in the past with full text, pinpoint searching. Link to case law cited within any court document via Fastcase.

Analytics At Your Fingertips



Learn what happened the last time a particular judge, opposing counsel or company faced cases similar to yours.

Advanced out-of-the-box PTAB and TTAB analytics are always at your fingertips.

API

Docket Alarm offers a powerful API (application programming interface) to developers that want to integrate case filings into their apps.

LAW FIRMS

Build custom dashboards for your attorneys and clients with live data direct from the court.

Automate many repetitive legal tasks like conflict checks, document management, and marketing.

FINANCIAL INSTITUTIONS

Litigation and bankruptcy checks for companies and debtors.

E-DISCOVERY AND LEGAL VENDORS

Sync your system to PACER to automate legal marketing.